Indian J. Pure Appl. Math., **50**(4): 953-969, December 2019
 DOI: 10.1007/s13226-019-0366-z

SKEW-SYMMETRIC CIRCULAR DISTRIBUTIONS AND THEIR STRUCTURAL PROPERTIES

Mojtaba Hatami and Mohammad Hossein Alamatsaz

Department of Statistics, University of Isfahan, Isfahan, 8174673441, *Iran*
e-mails: m.hatami.v@gmail.com; alamatho@sci.ui.ac.ir

(*Received* 13 *January* 2018; *accepted* 1 *October* 2018)

A general method of constructing a circular model is to apply transformation to its argument. In this paper, we propose a new transformation in order to construct a large class of new skew-symmetric circular models. We consider a symmetric unimodal distribution as our base model and provide general results for the modality, skewness and shape properties of the resulting circular distributions. The new class enfolds two well-known and common classes of unimodal symmetric and asymmetric circular distributions. The skewness parameter in the new class greatly improves the flexibility of our model to cover symmetric, asymmetric, unimodal and multimodal data. Further, we consider Wrapped Cauchy distribution as a special case for our base distribution and introduce the Skew-Symmetric Wrapped Cauchy (SSWC) distribution, discuss its sub-models and estimate its parameters by the maximum likelihood method. Finally, an application of SSWC distribution and its inferential methods are illustrated using two real data examples.

Key words : Circular statistics; argument transformation; unimodality; peakedness; skewness; wrapped Cauchy distribution.

1. Introduction

Circular or directional data arise in many diverse fields, such as Biology (movements of migrating animals), Geology (directions of joints and faults), etc. Such data are used to describe the direction or phenomena that are periodic in time. Most of the classical statistical models for circular data involve symmetric and unimodal distributions, such as the von Mises, Wrapped Cauchy, cardioid and Wrapped normal distributions [11, 15]. However, in practice, often data are asymmetric and bi- or multi-modal. In recent years, a large number of asymmetric models are introduced in [6, 8, 10, 13, 18, 20, 24]. In particular, [1, 7, 12] proposed skewed and multimodal circular models.

Abe *et al*. [2] obtained a skewed circular model by applying an argument transformation to Jones-Pewsey family. A general method of constructing a circular model is to apply transformation of its argument. Consider a random variable Θ with probability density function $f(\theta)$ and replace the argument θ by some function of θ, such as $H(\theta)$, to obtain a new distribution. Since function f is the probability density function of an absolutely continuous circular distribution if, and only if,

1. $f(\theta) \geq 0$ almost every where on $(-\infty, \infty)$
2. $f(\theta + 2\pi) = f(\theta)$ almost every where on $(-\infty, \infty)$
3. $\int_{-\pi}^{\pi} f(\theta) d\theta = 1$,

the function $H(\theta)$ should be selected so that the new function, $f(H(\theta))$, satisfies the first two conditions and to make the third condition valid, the normalizing constant must be recomputed. This approach was first applied to cardioid distribution by [17]. Cardioid distribution is defined by the density function

$$f_C(\theta) = \frac{1}{2\pi}(1 + \kappa \cos(\theta - \xi)), \ \ -\pi \leq \theta < \pi, \ 0 \leq \ \kappa \leq 1,$$

where κ and ξ are concentration and location parameters, respectively. Papakonstantinou [17] used functions $H_1(\theta) = \theta + \nu \ \sin(\theta)$ and $H_2(\theta) = \theta + \nu \ \cos(\theta)$, $-\infty < \nu < \infty$ to extend the shape characteristics of the cardioid distribution. He replaced $\cos(\theta - \xi)$ by $\cos(H_1(\theta - \xi))$ and $\cos(H_2(\theta - \xi))$ in cardioid distribution. The resulting distributions are called (by [2]) Papakonstantinou's symmetric extended cardioid (SEC) and Papakonstantinou's asymmetric extended cardioid (AEC) distributions, respectively. For instance, the density of SEC distribution is

$$f_{SEC}(\theta) = \frac{1}{2\pi(1 - \kappa J_1(\nu))}(1 + \kappa \cos(\theta - \xi + \nu \ \sin(\theta - \xi))), \ \ -\pi \leq \theta < \pi,$$

and $0 \leq \kappa \leq 1$, where $J_p(z)$ denotes the Bessel function of the first kind of order p [9],

$$J_p(z) = \int_0^{\pi} \cos(p\theta + z \ \sin(\theta)) d\theta, \ p = 0, \pm 1, \pm 2, \ \ldots.$$

This distribution was studied in considerably more depth by [3].

Batschelet's symmetric extended von Mises (SEvM) and Batschelet's asymmetric extended von Mises (AEvM) distributions were presented by Batschelet [4]. They are the results of replacing the term $\cos(\theta - \xi)$ by $\cos(H_1(\theta - \xi))$ and $\cos(H_2(\theta - \xi))$ in von Mises distribution, respectively. The class of Batschelet's symmetric extended von Mises distributions has been studied more extensively by Pewsey *et al*. [22].

Abe *et al*. [2] studied some general properties of distributions obtained using these two transformations on unimodal and symmetric distributions containing the term $\cos(\theta - \xi)$ in their densities. They showed that if the selected base distributions are unimodal and symmetric, then the resulting distributions in which the arguments are transformed by $H_1(\theta) = \theta - \xi + \nu \sin(\theta - \xi)$ are symmetric distributions. In particular, if $-1 < \nu < 1$, the resulting distributions are unimodal and more flat-topped (sharply peaked) than the base distributions and they are multimodal otherwise. But, the resulting distributions of transformation of the argument with function $H_2(\theta)$ are skew and unimodal if $-1 < \nu < 1$ and they are multimodal otherwise. Cos$(H_1(\theta))$ and $\cos(H_2(\theta))$ are called unimodal symmetric and unimodal asymmetric transformations, respectively, by Pewsey *et al*. [21]. Abe *et al*. [2] constructed and proposed the symmetric extended Jones-Pewsey (SEJP) and the asymmetric extended Jones-Pewsey (AEJP) family of distributions and studied their characteristics.

In this paper, we construct a more flexible skew-symmetric circular model by using the method of argument transformation which can deal with skewness as well as multimodality. The new family of distributions has a skewness parameter and two shape parameters which can be used to model both symmetric and asymmetric, unimodal or multimodal data with a very wide range of skewness and kurtosis behaviours.

The paper is organized as follows. In Section 2, we define a new transformation to construct a skew-symmetric circular model. Then, we shall provide very general results concerning modality, skewness and shape properties of the new model. In Section 3, we introduce the skew-symmetric Wrapped Cauchy distribution of circular distributions based on the new transformation introduced in Section 2. Then, we consider its special cases and also estimate parameters of the family by the maximum likelihood estimation method. Applications of the proposed model are considered in Section 4 using two real data sets. We conclude the paper with some final remarks in Section 5.

2. Proposed Transformation of Argument

In this section, to extend circular models to some general skew-symmetric circular models, we introduce the following argument transformation function:

$$H(\theta; \tau, \nu, \lambda) = \theta + \tau + \frac{\nu \sin(\theta)}{\lambda + \cos(\theta)},\ \nu \in \Re,\ \lambda \in (1, \infty),\ \ \tau \in [-\pi, \pi). \tag{1}$$

Clearly, if $\nu = k\lambda,\ k \in \Re$ and $\lambda \to \infty$, then (1) tends to $\theta + \tau + k \sin(\theta)$. Thus, the unimodal symmetric and the unimodal asymmetric transformations are special cases of $\cos(H(\theta - \xi; \tau, \nu, \lambda))$, i.e., when $\nu = k\lambda,\ \lambda \to \infty$ and $\tau = 0$ it reduces to the unimodal symmetric transformation and when $\nu = k\lambda,\ \lambda \to \infty$ and $\tau = \frac{\pi}{2}$ it reduces to the unimodal asymmetric transformation. Thus ν and λ are shape parameters that control both the shape and the modality of the distribution and τ is a skewness parameter which extends symmetric circular distributions to distributions with various shapes such as flat-topped, skew, sharply peaked, etc.

Let $f(\theta)$ denote a symmetric circular density so that for a function g it can be written as

$$f(\theta) = g(\cos(\theta - \xi)), \quad -\pi \leq \theta < \pi, \tag{2}$$

which is the case in many known circular distributions such as cardioid, power-of-cosine, Wrapped Cauchy, von Mises and Jones$-$Pewsey circular distributions. These are all symmetric and unimodal. We shall refer to function (2) as the base distribution. Now, replacing the argument $\cos(\theta - \xi)$ by $\cos(H(\theta - \xi; \tau, \nu, \lambda))$, we obtain

$$f_{(\tau,\nu,\lambda)}(\theta) = c^{-1}_{(\tau,\nu,\lambda)} g(\cos(H(\theta - \xi; \tau, \nu, \lambda))), \;\; -\pi \leq \theta < \pi, \tag{3}$$

where $c^{-1}_{(\tau,\nu,\lambda)}$ is a normalizing constant, which we refer to as skew-symmetric model. Note that, $H(\theta; \tau, \nu, \lambda)$ can also be defined for $\lambda \in (-\infty, -1)$, but because $f_{(\tau,\nu,\lambda)}(\theta + \pi) = f_{(\tau+\pi,\nu,-\lambda)}(\theta)$, we restrict our attention to the case $1 < \lambda < \infty$. Without loss of generality, in what follows we will assume that the location parameter, ξ, equals 0. The base circular distribution is obtained when $\tau = \nu = 0$, i.e., $f_{(0,0,\lambda)}(\theta) = f(\theta) = g(\cos(\theta))$. Hence, we can write

$$f_{(\tau,\nu,\lambda)}(\theta) = c^{-1}_{(\tau,\nu,\lambda)} f(\theta + \tau + \frac{\nu \, \sin(\theta)}{\lambda + \cos(\theta)}), \tag{4}$$

where $c_{(\tau,\nu,\lambda)} = \int_{-\pi}^{\pi} f(\theta + \tau + \frac{\nu \, \sin(\theta)}{\lambda+\cos(\theta)}) \, d\theta$. In the following section, we study general structural characteristics of the resulting distribution (3), such as its modality and skewness.

2.1 *Modality*

In this section, we discuss the modality of skew-symmetric distributions. Assume now that the symmetric circular density $f(\theta)$ is unimodal and its first derivative is continuous. Since the cosine function is even, $f(\theta)$ will have a mode at $\theta = 0$ and an antimode at $\theta = -\pi$.

***Theorem* 1** — *Density (4) is unimodal if, and only if,*

$$(\nu, \lambda) \in A = \{\{\nu > 0, \lambda \geq \nu + 1\} \cup \{-4 < \nu \leq 0, \lambda \geq 2/\sqrt{\nu + 4}\} \\ \cup \{\nu \leq -4, \lambda \geq -\nu - 1\}\}$$

and it is multimodal otherwise.

PROOF : Differentiating the density (4) with respect to θ, one obtains

$$f'_{(\tau,\nu,\lambda)}(\theta) \propto H'(\theta; \tau, \nu, \lambda) f'(H(\theta; \tau, \nu, \lambda)),$$

which is 0 when $H'(\theta;\tau,\nu,\lambda)=0$ or $f'(H(\theta;\tau,\nu,\lambda))=0$. First, let $f'(H(\theta;\tau,\nu,\lambda))=0$. Since

$$f'(H(\theta;\tau,\nu,\lambda))=-\sin(H(\theta;\tau,\nu,\lambda))g'(\cos(H(\theta;\tau,\nu,\lambda)))$$

and $f(\theta)$ is unimodal and $f'(\theta)=-sin(\theta)g'(\cos(\theta))$, it follows that $g'(\cos(\theta))>0,\ \ \forall\theta$. Hence, $g'(\cos(H(\theta;\tau,\nu,\lambda)))>0$ and consequently, $f'(H(\theta;\tau,\nu,\lambda))=0$ is equivalent to $\sin(H(\theta;\tau,\nu,\lambda))=0$ which happens when

$$H(\theta;\tau,\nu,\lambda)=j\pi\ \ (j=0,\pm1,\pm2,...),\ \forall\theta\in[-\pi,\pi). \tag{5}$$

Now, if $H'(\theta;\tau,\nu,\lambda)=0$, we have

$$H'(\theta;\tau,\nu,\lambda)=\frac{\cos^2(\theta)+\nu(2+\lambda)\cos(\theta)+\lambda^2+\nu}{(\lambda+\cos(\theta))^2}=0,$$

or, equivalently,

$$\cos^2(\theta)+\nu(2+\lambda)\cos(\theta)+\lambda^2+\nu=0. \tag{6}$$

We solve the quadratic form (6) for $y=\cos(\theta)$. Since its discriminant is $\Delta=\lambda^2\nu^2+4\nu(\lambda^2-1)$, there are three following situations:

(i) When $\Delta<0$, that is,

$$\{\Delta<0\}=\left\{\nu,\ \lambda|-4<\nu<0,\lambda>\ \frac{2}{\sqrt{\nu+4}}\right\},$$

there are no real roots for $H'(\theta;\tau,\nu,\lambda)$. Thus, the number of roots of $f'_{(\tau,\nu,\lambda)}(\theta)$ equals to the number of solutions in (5). In this case, $H(\theta;\tau,\nu,\lambda)$ is strictly increasing because $H'(\theta;\tau,\nu,\lambda)>0$ and since the range of $H(\theta;\tau,\nu,\lambda)$ belongs to $[\tau-\pi,\tau+\pi)$, then, equation (5) and therefore $f'_{(\tau,\nu,\lambda)}(\theta)=0$ have two roots. Thus $f_{(\tau,\nu,\lambda)}(\theta)$ will have a mode and an antimode.

(ii) When $\Delta=0$, that is,

$$\{\Delta=0\}=\left\{\nu,\ \lambda|\,\{\nu=0,1<\lambda<\infty\}\cup\{-4<\nu<0,\lambda=\ \frac{2}{\sqrt{\nu+4}}\}\right\},$$

the quadratic equation (6) has a root at $y=\frac{-\nu-2}{\sqrt{\nu+4}}$. Now, since function $H'(\theta;\tau,\nu,\lambda)$ is even (symmetric about zero), $H'(\theta;\tau,\nu,\lambda)$ has at most two roots. But, here, $H'(\theta;\tau,\nu,\lambda)\geq0$, therefore the number of roots of the function $f'_{(\tau,\nu,\lambda)}(\theta)$ is equal to those of (5). But, since $H(\theta;\tau,\nu,\lambda)$ is increasing, similar to (i), equation (5) has two solutions. Thus, $f_{(\tau,\nu,\lambda)}(\theta)$ is unimodal.

(iii) Finally, when $\Delta>0$, the quadratic equation (6) has two real solutions $y_1=-\frac{1}{2}\nu\lambda-\lambda-\frac{1}{2}\sqrt{\Delta}$ and $y_2=-\frac{1}{2}\nu\lambda-\lambda+\frac{1}{2}\sqrt{\Delta}$, provided that $y_1,y_2\notin[-1,1]$, that is

$$\{\nu,\ \lambda|\{\nu>0,\lambda\geq\nu+1\}\cup\{\nu<-3,\lambda\geq-\nu-1\}\}.$$

Hence, $H'(\theta;\tau,\nu,\lambda)$ has no roots, because $H'(\theta;\tau,\nu,\lambda) > 0$, i.e., $H(\theta;\tau,\nu,\lambda)$ is an increasing function. In such a case, equation (5) has two roots. Thus, $f_{(\tau,\nu,\lambda)}(\theta)$ will have a mode and an antimode. When at least one of the roots (y_1 or y_2) happens in the interval $[-1,1]$, $H'(\theta;\tau,\nu,\lambda)$ has two roots. So $H(\theta;\tau,\nu,\lambda)$ is not monotone and hence the number of the roots of (5) depends on the values of $H(\theta;\tau,\nu,\lambda)$ in the extreme points, in which case $f_{(\tau,\nu,\lambda)}(\theta)$ is multimodal. The set A contains all regions of the parameter space where the function $f_{(\tau,\nu,\lambda)}(\theta)$ is unimodal. This is highlighted in black in Figure 1 below. □

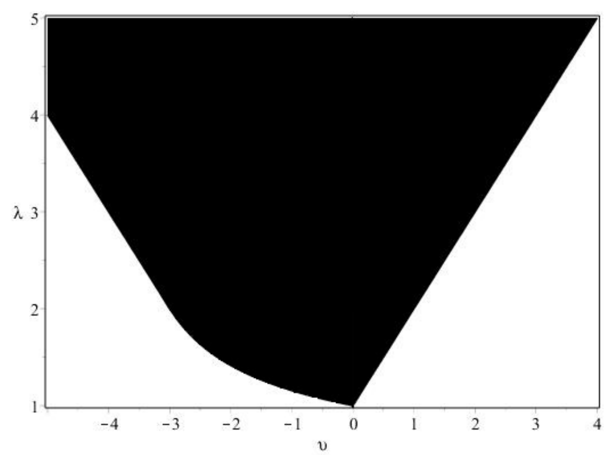

Figure 1 : The region highlighted in black shows (ν,λ)-values wherein the density (4) is unimodal.

When $f_{(\tau,\nu,\lambda)}(\theta)$ is unimodal, i.e., $(\nu,\ \lambda) \in A$, the mode is defined uniquely by $M = H^{-1}(0;\tau,\nu,\lambda)$. So, since $H(\theta;\tau,\nu,\lambda)$ is a monotone function, the value of the function at the mode is $f_{(\tau,\nu,\lambda)}(M) = c^{-1}_{(\tau,\nu,\lambda)} f(0)$.

2. *Skewness*

As mentioned earlier, to produce extended families of distributions containing symmetric densities which are more sharply peaked or flat-topped than the originals, Abe *et al*. [2] made use of unimodal symmetric transformation $\cos(H_1(\theta-\xi))$ and for skew families they made use of unimodal asymmetric transformation $\cos(H_2(\theta-\xi))$. But, in our model τ is a skewness parameter which actually controls symmetry and asymmetry of the distribution. When $\tau = 0$, $H(\theta;0,\nu,\lambda) = \theta + \frac{\nu\sin(\theta)}{\lambda+\cos(\theta)}$ is an odd function, so the density function $f_{(\tau,\nu,\lambda)}(\theta)$ is symmetric about $\theta = 0$. When $\tau = -\pi$,

$$f_{(-\pi,\nu,\lambda)}(\theta) = c^{-1}_{(-\pi,\nu,\lambda)} g(\cos(H(\theta;-\pi,\nu,\lambda)) = c^{-1}_{(\pi,\nu,\lambda)} g(-\cos(H(\theta;0,\nu,\lambda))$$

is symmetric about zero and has a mode at $\theta = -\pi$ and an antimode at $\theta = 0$. While if $\tau = \frac{\pi}{2}$, $\cos(H(\theta;\frac{\pi}{2},\nu,\lambda)) = \sin(H(\theta;0,\nu,\lambda))$ and, thus, the density function $f_{(\tau,\nu,\lambda)}(\theta)$ is skewed.

***Theorem* 2** — *Suppose that in (4),* $\tau \in (-\pi, 0]$ $(\tau \in (0, \pi))$ *with* $(\nu,\ \lambda) \in A$ *and* M *is the mode. Then, we have* $M \in [0, \pi)$ $(M \in (-\pi, 0))$.

PROOF : When $(\nu,\ \lambda) \in A$, $H(\theta; \tau, \nu, \lambda)$ is increasing, $H(-\pi; \tau, \nu, \lambda) = \tau - \pi$ and $H(\pi; \tau, \nu, \lambda) = \tau + \pi$. Since $\tau \in (-\pi, \pi)$, the function $H(\theta; \tau, \nu, \lambda)$ intersects the horizontal axis exactly at once. When $\tau = 0$ the point of intersection happens at $\theta = 0$ and if $\tau \in (-\pi, 0)$ $(\tau \in (0, \pi))$ the point of intersection is on the right (left) coordinate axes. Consequently, the mode is in the interval $(0, \pi)((-\pi, 0))$. □

In the following theorem, we show that τ is an effective parameter in kurtosis of $f_{(\tau,\nu,\lambda)}$.

***Theorem* 3** — *Let* $|\tau_1| < |\tau_2|$ *and* $(\nu,\ \lambda) \in A$*, then we have:*

(i) $f_{(\tau_1,\nu,\lambda)}(M_1) > f_{(\tau_2,\nu,\lambda)}(M_2)$, *if* $\nu > 0$

(ii) $f_{(\tau_1,\nu,\lambda)}(M_1) < f_{(\tau_2,\nu,\lambda)}(M_2)$, *if* $\nu < 0$.

where M_i*'s are the modes corresponding to density functions* $f_{(\tau_i,\nu,\lambda)}(\theta)$, $i = 1, 2$.

PROOF Since $f_{(\tau,\nu,\lambda)}(-\theta) = f_{(-\tau,\nu,\lambda)}(\theta)$, we have $c_{(\tau,\nu,\lambda)} = c_{(-\tau,\nu,\lambda)}$. Thus, without loss of generality, we assume that $\tau > 0$. As seen before, $f_{(\tau_i,\nu,\lambda)}(M_i) = c^{-1}{}_{(\tau_i,\nu,\lambda)} f(g(1))$. We also note that

$$\frac{d}{d\tau} c_{(\tau,\nu,\lambda)} = \int_{-\pi}^{\pi} -\sin(H(\theta; \tau, \nu, \lambda)) g'(\cos(H(\theta; \tau, \nu, \lambda)))\, d\theta,$$

or, by putting $H(\theta; \tau, \nu, \lambda) = u$, it becomes

$$= \int_{\tau-\pi}^{\tau+\pi} -\sin(u) g'(\cos(u)) \frac{1}{H'(H^{-1}(u; \tau, \nu, \lambda))}\, d\theta.$$

Since the integrand is 2π-periodic, we obtain

$$\frac{d}{d\tau} c_{(\tau,\nu,\lambda)} = \int_{-\pi}^{\pi} -\sin(u) g'(\cos(u)) \frac{1}{H'(H^{-1}(u; \tau, \nu, \lambda))}\, d\theta,$$

$$= \int_{0}^{\pi} \sin(u) g'(\cos(u)) \left(\frac{1}{H'(H^{-1}(-u; \tau, \nu, \lambda))} - \frac{1}{H'(H^{-1}(u; \tau, \nu, \lambda))} \right) d\theta,$$

where

$$\frac{1}{H'(\theta; \tau, \nu, \lambda)} = \frac{(\lambda + \cos(\theta))^2}{\cos{(\theta)}^2 + \lambda(\nu + 2)\cos(\theta) + \nu + \lambda^2}.$$

Now define

$$k(u) = \frac{1}{H'(H^{-1}(-u; \tau, \nu, \lambda))} - \frac{1}{H'(H^{-1}(u; \tau, \nu, \lambda))}.$$

Since $g(\cos(u))$ is unimodal at $u = 0$, we have $\sin(u)g'(\cos(u)) > 0$ on $(0, \pi)$. We, thus, need only to know the sign of $k(u)$ on the interval $(0, \pi)$. First, we find the roots of $k(u)$, i.e., the solutions of

$$H'(H^{-1}(-u; \tau, \nu, \lambda)) = H'(H^{-1}(u; \tau, \nu, \lambda)).$$

Since $H'(u; \tau, \nu, \lambda)$ is $2\pi-$periodic, this yields

$$H^{-1}(-u; \tau, \nu, \lambda) = H^{-1}(u; \tau, \nu, \lambda) + 2k\pi,$$

or equivalently,

$$-u = H(H^{-1}(u; \tau, \nu, \lambda) + 2k\pi; \tau, \nu, \lambda),$$

and consequently $u = -k\pi$. Thus, $k(u)$ is either positive or negative on the interval $(0, \pi)$. Note that as mentioned in the proof of Theorem 1, $H'(\theta; \tau, \nu, \lambda)$ has no real roots when $(\nu,\ \lambda) \in A$.

Now to prove part (i), let $\nu > 0$. Thus, the function $\frac{1}{H'(\theta;\tau,\nu,\lambda)}$ has a maximum at $(2j + 1)\pi$ $(j = 0, \pm1, \pm2, ...)$. Since the maximum of $\frac{1}{H'(H^{-1}(-u;\tau,\nu,\lambda))}$ is at $u = \pi - \tau$, inside of $(0, \pi)$, but the maximum of $\frac{1}{H'(H^{-1}(u;\tau,\nu,\lambda))}$ is at $u = \tau + \pi$, outside of $(0, \pi)$, we have

$$\frac{1}{H'(H^{-1}(-(\pi - \tau); \tau, \nu, \lambda))} > \frac{1}{H'(H^{-1}(\pi - \tau; \tau, \nu, \lambda))},$$

i.e., $k(u) > 0$, $\forall u \in (0, \pi)$ and thus $\frac{d}{d\tau} c_{(\tau,\nu,\lambda)} > 0$. Equivalently, $c_{(\tau_1,\nu,\lambda)} < c_{(\tau_2,\nu,\lambda)}$ and consequently we have $f_{(\tau_1,\nu,\lambda)}(M_1) > f_{(\tau_2,\nu,\lambda)}(M_2)$.

For part (ii), i.e., when $\nu < 0$, $\frac{1}{H'(\theta;\tau,\nu,\lambda)}$ takes its minimum at $(2j + 1)\pi$ $(j = 0, \pm1, \pm2, ...)$. Thus, it follows that

$$\frac{1}{H'(H^{-1}(-(\pi - \tau); \tau, \nu, \lambda))} < \frac{1}{H'(H^{-1}(\pi - \tau; \tau, \nu, \lambda))}.$$

Hence, $k(u) < 0,\ \forall u \in (0, \pi)$ and, therefore, $\frac{d}{d\tau} c_{(\tau,\nu,\lambda)} < 0$ or, equivalently, $c_{(\tau_1,\nu,\lambda)} > c_{(\tau_2,\nu,\lambda)}$. Consequently, we obtain $f_{(\tau_1,\nu,\lambda)}(M_1) < f_{(\tau_2,\nu,\lambda)}(M_2)$. □

2.3 *Shape properties*

In addition to the assumptions of Section 2.1 on f, here we further assume that the second derivative of $f(\theta)$, $f''(\theta)$, exists and is continuous. The following theorem contains useful conditions under which the peakedness and flatness of the density (4) can be controlled.

Theorem 4 — *For the density (4) with $\tau = 0$ and $(\nu,\ \lambda) \in A$, we have:*

a) *If $\nu_1 < \nu_2$ then $f_{(0,\nu_1,\lambda)}(0) < f_{(0,\nu_2,\lambda)}(0)$ and $f_{(0,\nu_1,\lambda)}(-\pi) < f_{(0,\nu_2,\lambda)}(-\pi)$*

b) *If* $\nu > 0$ *and* $\lambda_1 < \lambda_2$ *then* $f_{(0,\nu,\lambda_1)}(0) > f_{(0,\nu,\lambda_2)}(0)$ *and* $f_{(0,\nu,\lambda_1)}(-\pi) > f_{(0,\nu,\lambda_2)}(-\pi)$

c) *If* $\nu < 0$ *and* $\lambda_1 < \lambda_2$ *then* $f_{(0,\nu,\lambda_1)}(0) < f_{(0,\nu,\lambda_2)}(0)$ *and* $f_{(0,\nu,\lambda_1)}(-\pi) < f_{(0,\nu,\lambda_2)}(-\pi)$

d) *If* $\nu_1 < \nu_2$ *then* ${f''}_{(0,\nu_1,\lambda)}(0) > {f''}_{(0,\nu_2,\lambda)}(0)$ *and* ${f''}_{(0,\nu_1,\lambda)}(-\pi) > {f''}_{(0,\nu_2,\lambda)}(-\pi)$

e) *If* $\nu > 0$ *and* $\lambda_1 < \lambda_2$ *then* ${f''}_{(0,\nu,\lambda_1)}(0) < {f''}_{(0,\nu,\lambda_2)}(0)$ *and* ${f''}_{(0,\nu,\lambda_1)}(-\pi) < {f''}_{(0,\nu,\lambda_2)}(-\pi)$

f) *If* $\nu < 0$ *and* $\lambda_1 < \lambda_2$ *then* ${f''}_{(0,\nu,\lambda_1)}(0) > {f''}_{(0,\nu,\lambda_2)}(0)$ *and* ${f''}_{(0,\nu,\lambda_1)}(-\pi) > {f''}_{(0,\nu,\lambda_2)}(-\pi)$.

PROOF : (a). Note that $f_{(\tau,\nu,\lambda)}(\theta)$ is unimodal when $(\nu,\ \lambda) \in A$ and because $\tau = 0$, the unique mode happens at $\theta = 0$. Thus, $f_{(\tau,\nu,\lambda)}(\theta)$ is strictly decreasing on the interval $(0,\ \pi)$. So, since for all $0 < \theta < \pi$, $0 < \theta + \frac{\nu\,\sin(\theta)}{\lambda+\cos(\theta)} < \pi$ and $\theta + \frac{\nu_1\,\sin(\theta)}{\lambda+\cos(\theta)} < \theta + \frac{\nu_2\,\sin(\theta)}{\lambda+\cos(\theta)}$,

$$c_{(0,\nu_1,\lambda)} = 2\int_0^{\pi} f(\theta + \frac{\nu_1\,\sin(\theta)}{\lambda+\cos(\theta)})\,d\theta > 2\int_0^{\pi} f(\theta + \frac{\nu_2\,\sin(\theta)}{\lambda+\cos(\theta)})\,d\theta = c_{(0,\nu_2,\lambda)},$$

and, thus,

$$f_{(0,\nu_1,\lambda)}(0) = c^{-1}_{(0,\nu_1,\lambda)} f(0) < c^{-1}_{(0,\nu_2,\lambda)} f(0) = f_{(0,\nu_2,\lambda)}(0).$$

Similarly, we can show that $f_{(0,\nu_1,\lambda)}(-\pi) < f_{(0,\nu_2,\lambda)}(-\pi)$. (b) and (c) are proved similarly.

(d) Since $f_{(0,\nu,\lambda)}(\theta)$ is symmetric and unimodal at $\theta = 0$, we have ${f'}_{(0,\nu,\lambda)}(0) = 0$ and ${f''}_{(0,\nu,\lambda)}(0) < 0$. Now,

$${f'}_{(\tau,\nu,\lambda)}(\theta) = c^{-1}_{(\tau,\nu,\lambda)} H'(\theta;\tau,\nu,\lambda) f'(H(\theta;\tau,\nu,\lambda))$$

and

$$\begin{aligned}{f''}_{(\tau,\nu,\lambda)}(\theta) &= c^{-1}_{(\tau,\nu,\lambda)} H''(\theta;\tau,\nu,\lambda) f'(H(\theta;\tau,\nu,\lambda)) \\ &\quad + c^{-1}_{(\tau,\nu,\lambda)} {H'}^2(\theta;\tau,\nu,\lambda) f''(H(\theta;\tau,\nu,\lambda)),\end{aligned}$$

thus, we obtain

$${f''}_{(0,\nu,\lambda)}(0) = c^{-1}_{(0,\nu,\lambda)} f''(0)(1 + \frac{\nu}{1+\lambda})^2 < 0.$$

Consequently, it follows that ${f''}_{(0,\nu_1,\lambda)}(0) > {f''}_{(0,\nu_2,\lambda)}(0)$. Similarly, we can see that ${f''}_{(0,\nu_1,\lambda)}(-\pi) > {f''}_{(0,\nu_2,\lambda)}(-\pi)$. The proofs of parts (e) and (f) are similar and thus omitted. □

The curvature of $f_{(\tau,\nu,\lambda)}(\theta)$ at θ equals $\frac{{f''}_{(\tau,\nu,\lambda)}(\theta)}{\left(1+({f'}_{(\tau,\nu,\lambda)}(\theta))^2\right)^{\frac{3}{2}}}$. Thus, at the mode, $\theta = M$, ${f'}_{(\tau,\nu,\lambda)}(M) = 0$ and the curvature is equal to ${f''}_{(\tau,\nu,\lambda)}(M)$. Given the results above, $(\nu,\ \lambda)$ are clearly shape parameters which control the peakedness or flat-toppedness properties of the density. For example, if $\tau = 0$ and conditions **(a)** and **(b)** are satisfied, we will say that $f_{(0,\nu_1,\lambda)}$ is more flat-topped than $f_{(0,\nu_2,\lambda)}$ and also $f_{(0,\nu_2,\lambda)}$ has heavier tails than $f_{(0,\nu_1,\lambda)}$.

3. SKEW-SYMMETRIC EXTENSION OF THE WRAPPED CAUCHY DISTRIBUTION

In this section, we consider the Wrapped Cauchy distribution which is an important two-parameter symmetric unimodal circular distribution which suggests itself as a suitable candidate for a base distribution. We apply the general construction of Section 2 to produce a skew-symmetric extension of this distribution.

We provide results for shape characteristics of this distribution and discuss maximum likelihood estimation of its parameters. The density of a Wrapped Cauchy distribution is

$$f_{WC}(\theta) = \frac{1}{2\pi}\frac{1-r^2}{1+r^2-2r\cos(\theta-\xi)}, \quad -\pi \leq \theta < \pi, \tag{7}$$

where ξ is a location parameter and $0 \leq r \leq 1$ is a concentration parameter.

Replacing $\cos(\theta-\xi)$ by $\cos(H(\theta-\xi;\tau,\nu,\lambda))$ in Wrapped Cauchy density (7) results in what we shall call the skew-symmetric Wrapped Cauchy (SSWC) family of distributions with density

$$f_{SSWC}(\theta) = c^{-1}_{(r,\tau,\nu,\lambda)}\left\{1+r^2-2r\cos(\theta-\xi+\tau+\frac{\nu\sin(\theta-\xi)}{\lambda+\cos(\theta-\xi)})\right\}^{-1}, \tag{8}$$

where

$$c_{(r,\tau,\nu,\lambda)} = \int_{-\pi}^{\pi}\left\{1+r^2-2r\cos(\theta-\xi+\tau+\frac{\nu\sin(\theta-\xi)}{\lambda+\cos(\theta-\xi)})\right\}^{-1}d\theta$$

must generally be computed numerically. Some important special cases of the SSWC distribution are listed here:

(i) when $\nu = 0$, (8) reduces to the Wrapped Cauchy density (7). In this case we consider $\tau = 0$.

(ii) when $\tau = 0$, it reduces to a symmetric Wrapped Cauchy distribution with density

$$f_{SWC}(\theta) = c^{-1}_{(r,0,\nu,\lambda)}\left\{1+r^2-2r\cos(\theta-\xi+\frac{\nu\sin(\theta-\xi)}{\lambda+\cos(\theta-\xi)})\right\}^{-1}.$$

(iii) when $\tau = \pi/2$, an asymmetric Wrapped Cauchy distribution with density

$$f_{AWC}(\theta) = c^{-1}_{(r,\pi/2,\nu,\lambda)}\left\{1+r^2-2r\sin(\theta-\xi+\frac{\nu\sin(\theta-\xi)}{\lambda+\cos(\theta-\xi)})\right\}^{-1}$$

is obtained.

The flexibility of unimodal cases of SSWC densities are partially portrayed in Figure 2. It can be seen that the parameter τ controls asymmetry of the densities. In particular, multimodal cases of SSWC densities are shown in Figure 3.

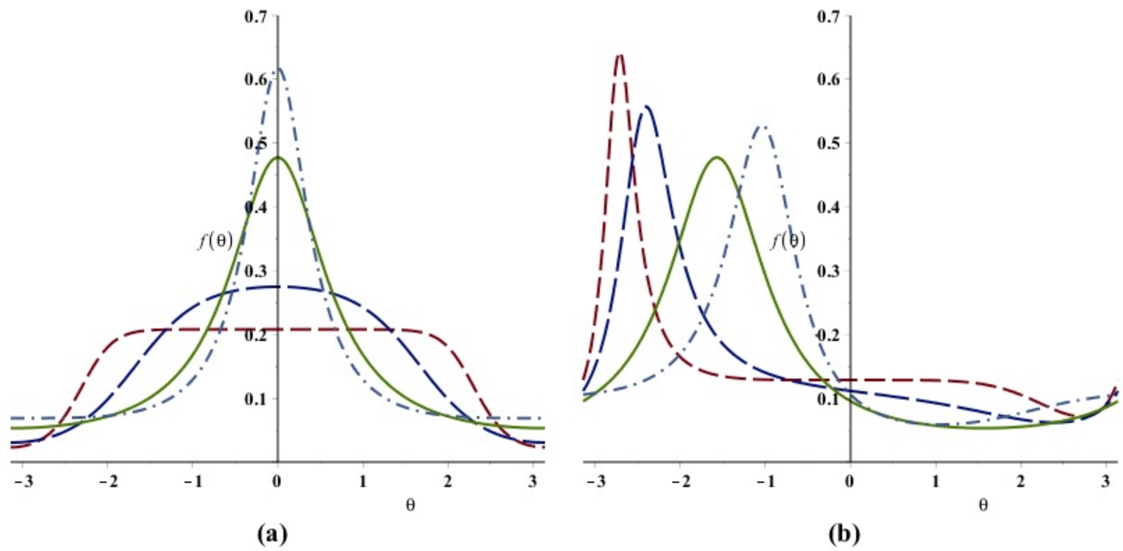

Figure 2: Unimodal SSWC densities with $\xi = 0$ and $r = 0.5$ for (a) $\tau = 0$ and (b) $\tau = \pi/2$. In each panel: $\nu = 0$ (solid curve); $\nu = -3, \lambda = 2$ (dashed curve); $\nu = -4, \lambda = 4$ (long dashed curve); $\nu = 4, \lambda = 6$ (dash-dotted curve).

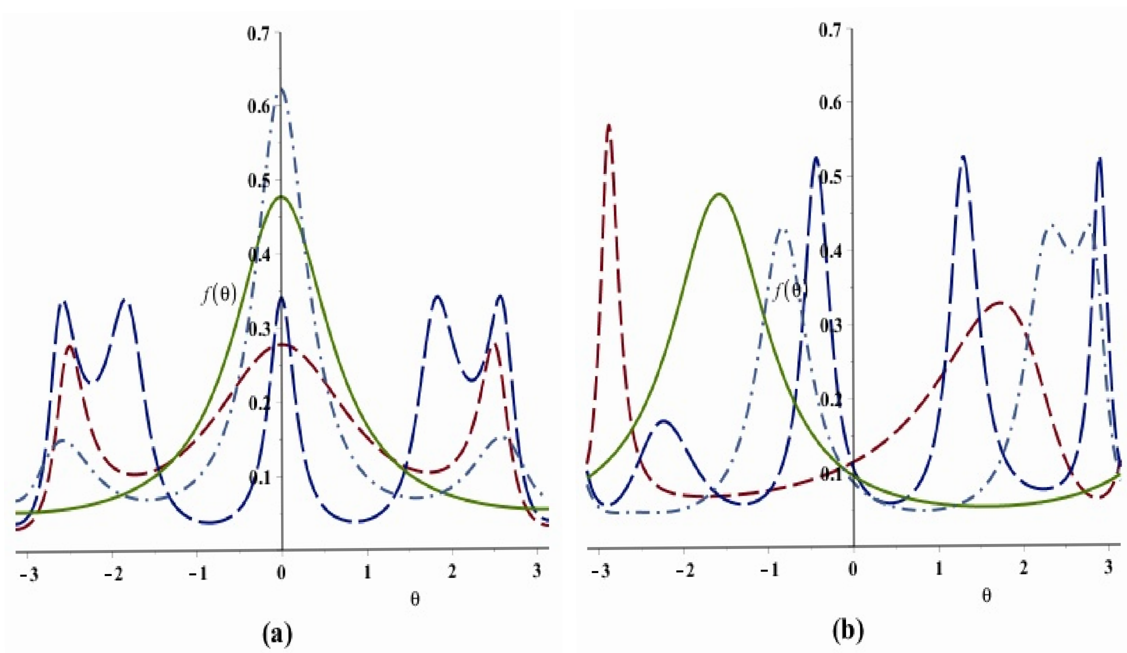

Figure 3: Multimodal SSWC densities with $\xi = 0$ and $r = 0.5$ for (a) $\tau = 0$ and (b) $\tau = \pi/2$. In each panel: $\nu = 0$ (solid curve); $\nu = -5, \lambda = 2$ (dashed curve); $\nu = 8$, $\lambda = 2$ (long dashed curve); $\nu = 2, \lambda = 1.3$ (dash-dotted curve).

3.1 *Maximum Likelihood Estimation*

Inference for parameters of SSWC distribution can be performed by the maximum likelihood method. Let $\theta_1, ..., \theta_n$ be a random sample of size n from the distribution SSWC. Then, the log-likelihood function is

$$l(\xi, r, \tau, \nu, \lambda) = -n \log c_{(r,\tau,\nu,\lambda)} - \sum_{i=1}^{n} \log \left(1 + r^2 - 2r\cos(\theta_i - \xi + \tau + \frac{\nu \sin(\theta_i - \xi)}{\lambda + \cos(\theta_i - \xi)})\right).$$

Taking partial derivatives from the log-likelihood function with respect to ξ, r, τ, ν and λ, respectively, and equating the resulting expressions to zero yield likelihood equations. The estimates can be obtained by means of numerical procedures. Function `optim` in program R provides the nonlinear optimization routine for solving such problems. We make use of **L-BFGS-B** optimisation method in the following illustrative examples in Section 4. In the case of grouped data, suppose that there are m class intervals, $(\theta_0, \theta_1), ..., (\theta_{m-1}, \theta_m)$, where $\theta_0 = 0$ and $\theta_m = 2\pi$. Denoting the number of data values in the jth class interval by n_j and thus a total of $n = n_1 + n_2 + ... + n_m$ observations, the log-likelihood function is given by

$$l(\xi, r, \tau, \nu, \lambda) = -n \log c_{(r,\tau,\nu,\lambda)} - \sum_{j=1}^{m} n_j \int_{\theta_{j-1}}^{\theta_j} \log \left(1 + r^2 - 2r\cos(\theta - \xi + \tau + \frac{\nu \sin(\theta - \xi)}{\lambda + \cos(\theta - \xi)})\right) d\theta.$$

The maximization of this function can also be achieved using the optimization options available in R referred to above.

4. Applications

In this section, we apply the models described in Section 3 to analyse two real circular data sets.

4.1 *Thunder data*

We consider the grouped data set of size n = 725, in Table 1.3 of [14], which is adapted from Bishop [5]. The data measure the number of occasions on which thunder was heard during each two hourly intervals of the day at Kew (England) during summer from 1910-1935. The data were recorded and grouped into two-hourly intervals of a day, then converted into angles.

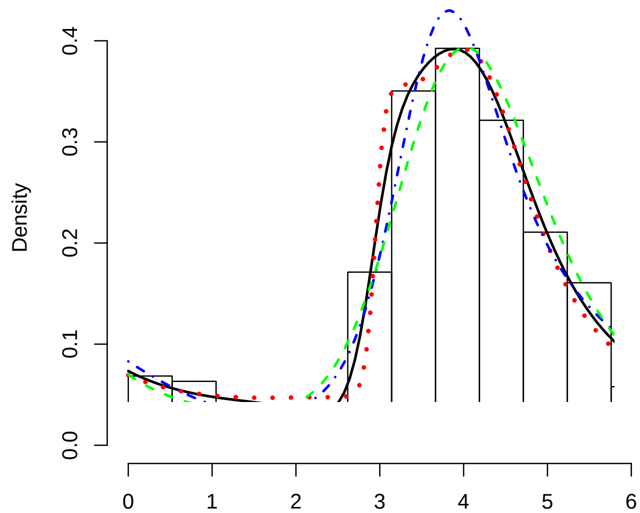

Figure 4: Histogram of the thunder data represented in radians, together with the densities of the maximum likelihood fits for the skew-symmetric Wrapped Cauchy (solid curve), asymmetric Wrapped Cauchy (dotted curve), asymmetric extended Jones-Pewsey (dash-dotted curve) and sine-skewed Jones-Pewsey (dashed curve) distributions.

In Figure 4, the histogram of the data set is illustrated, which reveals that the distribution is asymmetric. Also, the test of Pewsey [19], with a p-value of 0.0000, rejects the underlying distribution as being symmetric emphatically. In Table 1, we present the maximum likelihood estimates, the values of the maximized log-likelihood (MLL), Akaike information criterion (AIC) and Bayesian information criterion (BIC), together with the p-values for the chi-squared goodness-of-fit test of the skew-symmetric Wrapped Cauchy, the asymmetric Wrapped Cauchy, sine-skewed Jones-Pewsey (SineSJP) models of Abe and Pewsey [1], the asymmetric extended Jones-Pewsey (AEJP) distribution of Abe *et al*. [2] and the generalized t model (GT) of Siew *et al*. [23]. The fitted skew-symmetric densities are superimposed over the histogram of the data set in Figure 4. It can be seen from Table 1 that the skew-symmetric Wrapped Cauchy distribution has the highest MLL value and lowest AIC value. But based on BIC criterion, asymmetric Wrapped Cauchy density provides the best fit. Considering the MLL values for the SSWC and AWC distributions, the test statistic for the usual likelihood-ratio test is calculated to be 2(-1580.79+1582.16) = 2.74. Comparing this value with the quantiles of the χ^2_1 distribution, the p-value of the test is 0.097. Thus, the skew-symmetric Wrapped Cauchy distribution does not provide a significant improvement comparing to the asymmetric Wrapped Cauchy distribution. Moreover, the p-values for the chi-squared goodness-of-fit test indicate that neither AEJP nor GT distributions provide a adequate fit to the data but the skew-symmetric Wrapped Cauchy and asymmetric Wrapped Cauchy models provide perfectly reasonable fits to the data.

Table 1: Maximum likelihood estimates, the values of the maximized log-likelihood (MLL), Akaike information criterion (AIC), Bayesian information criterion (BIC), and p-value for the chi-squared goodness-of-fit test for the fits to the thunder data of the skew-symmetric Wrapped Cauchy (SSWC), asymmetric Wrapped Cauchy (AWC), sine-skewed Jones-Pewsey (SineSJP), asymmetric extended Jones-Pewsey (AEJP) and the generalized t (GT) models.

Model						MLL	AIC	BIC	$p(g\text{-}o\text{-}f)$
	$\hat{\xi}$	$\hat{r}$	$\hat{\nu}$	$\hat{\tau}$	$\hat{\lambda}$				
SSWC	5.60	0.56	-0.88	0.92	1.24	-1580.79	3171.58	3194.51	0.25
	$\hat{\xi}$	$\hat{r}$	$\hat{\nu}$	$\hat{\lambda}$					
AWC	5.97	0.49	-0.28	1.04	-	-1582.16	3172.32	3190.67	0.14
	$\hat{\xi}$	$\hat{\kappa}$	$\hat{\psi}$	$\hat{\nu}$					
AEJP	2.72	1.31	-0.08	0.52	-	-1584.72	3177.43	3195.78	0.04
	$\hat{\xi}$	$\hat{\kappa}$	$\hat{\psi}$	$\hat{\lambda}$					
SineSJP	3.55	0.94	-0.84	0.68	-	-1584.24	3176.48	3194.83	0.05
	$\hat{\xi}_1$	$\hat{\xi}_2$	$\hat{\kappa}_1$	$\hat{\kappa}_2$	$\hat{\psi}$				
GT	4.15	3.91	1.49	0.45	0.71	-1584.27	3178.55	3201.48	0.02

Approximate 95% confidence intervals for the parameters ξ, r, ν, τ and λ of the SSWC distribution, calculated from their individual profile log-likelihood functions together with standard chi-squared theory, are (5.27, 6.62), (0.47, 0.64), (-1.45, -0.25), (0.59 ,1.62) and (1.05, 1.80), whilst those calculated using the observed information matrix and standard asymptotic normal theory are (5.06, 6.14), (0.43, 0.67), (-1.75, -0.02), (0.25, 1.59) and (0.85, 1.63). The fact that two intervals for τ contain the value $\pi/2$ show that AWC distribution is a potential model for the data.

From the results in Table 1, it can be seen that among models considered with four parameters the asymmetric Wrapped Cauchy distribution has the highest MLL, lowest AIC and BIC values. Thus, the asymmetric Wrapped Cauchy distribution provides a better fit to the data than the other two skew four parameters models.

4.2 *Wind direction data*

As our second example we consider a grouped frequency data set taken from Mardia [14]. The data represent wind directions at Crawley (England) for the 25 months, November-March, 1957-1961. The data is bimodal , implying two opposite regimes of wind direction. Consistent with these findings, the large-sample test of Pewsey [19], with a p-value 0, and the histogram in Figure 5 are suggestive of an underlying asymmetric bimodal circular distribution.

Table 2: Maximum likelihood estimates, values of the maximized log-likelihood (MLL), Akaike information criterion (AIC), Bayesian information criterion (BIC), and p-value for the chi-squared goodness-of-fit test for the fits to the wind direction data of SSWC, AWS, MvM and GT models.

Model						MLL	AIC	BIC	$p(g\text{-}o\text{-}f)$
	$\hat{\xi}$	$\hat{r}$	$\hat{\nu}$	$\hat{\tau}$	$\hat{\lambda}$				
SSWC	0.06	0.37	-11.18	1.16	9.29	-1813.60	3637.21	3659.56	0.19
	$\hat{\xi}$	$\hat{r}$	$\hat{\nu}$	$\hat{\lambda}$					
AWC	0.31	0.33	-10.86	9.48	-	-1816.29	3640.58	3658.46	0.05
	$\hat{\xi}_1$	$\hat{\xi}_2$	$\hat{\kappa}_1$	$\hat{\kappa}_2$	$\hat{p}$				
MvM	0.27	4.22	0.52	3.95	0.67	-1815.49	3640.99	3663.34	0.07
	$\hat{\xi}_1$	$\hat{\xi}_2$	$\hat{\kappa}_1$	$\hat{\kappa}_2$	$\hat{\psi}$				
GT	5.05	1.05	0.43	0.41	0.06	-1816.23	3642.46	3664.81	0.04

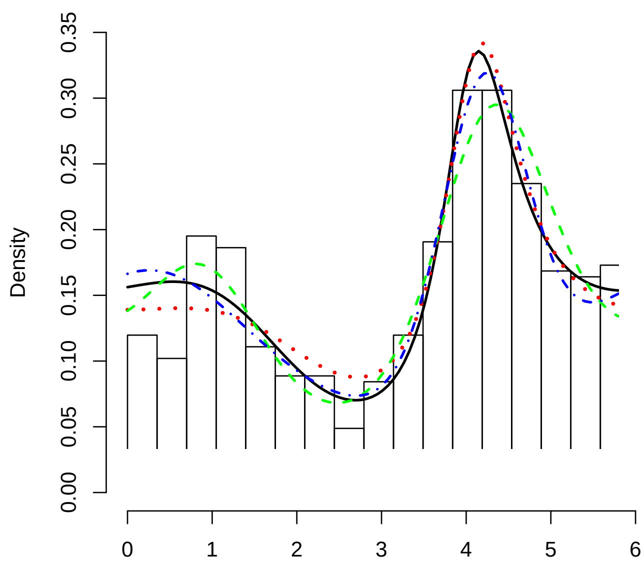

Figure 5: Histogram of the wind direction data (in radians), together with the densities of the maximum likelihood fits for the skew-symmetric Wrapped Cauchy (solid curve), asymmetric Wrapped Cauchy (dotted curve), Mixture von Mises (dash—dotted curve) and generalized t (dashed curve) distributions.

Table 2 presents the equivalent results to those presented in Table 1 for the wind direction data of the SSWC model, its AWC submodel and the generalized t (GT) model and mixture of two von Mises distribution (MvM). The AIC and MLL values identify the SSWC fit as providing the most parsimonious model for the data. The densities of the four fits are superimposed upon a linear histogram of the data in Figure 5. To compare the MLL values for these two fits using a likelihood ratio test, the test statistic is calculated to be 2(-1813.60 + 1816.29) = 5.38 (p-value=0.02). Thus, the SSWC distribution provide a significant improvement over its AWC submodel. But, based on BIC criterion, AWC density provides the best fit. The p-values for the chi-squared goodness-of-fit test indicate that SSWC model provides adequate fit to the data.

5. Conclusions

In this paper, we introduced a flexible class of skew-symmetric circular models by using the method of transformation of argument which contains the two well-known and common classes of unimodal symmetric and asymmetric circular models. It provides distributions with greater modelling flexibility than alternative models. Some general structural properties of our model such as modality, skewness and its shape were studied. We showed that this family can model skew-symmetric circular distributions. They are especially suitable in providing suitable models for both symmetric and asymmetric multimodal data.

Acknowledgement

The first author is grateful to the Graduate Office of the University of Isfahan, Iran for their support.

References

1. T. Abe and A. Pewsey, Sine-skewed circular distributions, *Statist. Papers*, **52** (2011), 683-707.
2. T. Abe, A. Pewsey, and K. Shimizu, Extending circular distributions through transformation of argument, *Ann. Inst. Statist. Math.*, **65** (2013), 833-858.
3. T. Abe, K. Shimizu, and A. Pewsey, On Papakonstantinous extension of the cardioid distribution, *Statist. Probab. Lett.*, **79** (2009), 2138-2147.
4. E. Batschelet, *Circular statistics in biology*, Academic Press, London, 1981.
5. B. V. Bishop, The frequency of thunderstorms at Kew observatory, *Met. Mag.*, **76** (1947), 108-111.
6. J. J. Fernández-Durán, Circular distributions based on nonnegative trigonometric sums, *Biometrics*, **60** (2004), 499-503.
7. E. Hernández-Sánchez and B. Scarpa, A wrapped flexible generalized skewnormal model for a bimodal circular distribution of wind directions, *Chil. J. Statist.*, **3** (2012), 131-143.
8. R. Gatto and S. R. Jammalamadaka, The generalized von Mises distribution, *Stat. Methodol.*, **4** (2007), 341-353.
9. I. S. Gradshteyn and I. M. Ryzhik, *Tables of integrals, series, and products*, 7nd edn, Academic Press, San Diego, 2007.

10. S. R. Jammalamadaka and T. J. Kozubowski, New families of wrapped distributions for modeling skew circular data, *Comm. Statist. Theory Methods*, **33** (2004), 2059-2074.
11. S. R. Jammalamadaka and A. SenGupta, *Topics in circular statistics*, World Scientific, Singapore, 2001.
12. S. Kato and M. C. Jones, A family of distributions on the circle with links to, and applications arising from, Möbius transformation, *Amer. Statist. Assoc.*, **105** (2010), 249-262.
13. S. Kim and A. SenGupta, A three parameter generalized von Mises distribution, *Statist. Papers*, **54** (2013), 685-693.
14. K. V. Mardia, *Statistics of directional data*, Academic Press, New York, 1972.
15. K. V. Mardia and P. E. Jupp, *Directional Statistics*, John Wiley, Chichester, 1999.
16. J. A. Mooney, P. J. Helms, and I. T. Jolliffe, Fitting mixtures of von mises distributions: A case study involving sudden infant death syndrome, *Comput. Statist. Data Anal.*, **41** (2003), 505-513.
17. V. Papakonstantinou, *Beiträge zur zirkulären Statistik*, Ph.D. thesis, University of Zurich, Switzerland, 1979.
18. A. Pewsey, The wrapped skew-normal distribution on the circle, *Comm. Statist: Theory Methods*, **29** (2000), 2459-2472.
19. A. Pewsey, Testing circular symmetry, *Canad. J. Statist.*, **30** (2002), 591-600.
20. A. Pewsey, The wrapped stable family of distributions as a flexible model for circular data, *Comput. Statist. Data Anal.*, **52** (2008), 1516-1523.
21. A. Pewsey, M. Neuhäuser, and G. D. Ruxton, *Circular statistics in R*, Oxford University Press, Croydon, 2013.
22. A. Pewsey, K. Shimizu, and R. de la Cruz, On an extension of the von Mises distribution due to Batschelet, *J. Appl. Stat.*, **38** (2011), 1073-1085.
23. H. Y. Siew, S. Kato, and K. Shimizu, Generalized *t*-distribution on the circle, *Jpn. J. Appl. Stat*., **37** (2008), 1-16.
24. D. Umbach and S. R. Jammalamadaka, Building asymmetry into circular distributions, *Statist. Probab. Lett.*, **79** (2009), 659-663.